https://ntrs.nasa.gov/search.jsp?R=19660010840 2020-03-16T22:39:52+00:00Z

Second Quarterly Report

"Analytical Procedure for Determining Random Load Acting on a Spacecraft Due to a Primary Random Load Acting on an Exterior Structure"

(1 September 1965 - 30 November 1965)

Contract No: NAS5-9601

Prepared by:

Richard H. Lyon
Jerome E. Manning

Bolt Beranek and Newman Inc.
50 Moulton Street
Cambridge Massachusetts 02138

for

Goddard Space Flight Center
Greenbelt, Maryland

TABLE OF CONTENTS

GLOSSARY OF SYMBOLS

A_i = area of i^{th} item

c_i = material longitudinal wavespeed in i^{th} item

$c_F^{(i)}$ = flexural wavespeed of i^{th} item

c_s = shear wavespeed

$c_T^{(i)}$ = torsional wavespeed of i^{th} item (where appropriate)

E_i = total energy of i^{th} item

$\mathcal{E}_i$ = modal energy of i^{th} item

F,T = as subscripts or superscripts, referring to flexural or torsional motion.

H_4 = thickness of spacecraft sandwich wall

J = beam torsional inertial constant

K = beam torsional stiffness coefficient

$k_F^{(i)}$ = flexural wavenumber of i^{th} item

log = logarithm to base 10

ℓn = natural logarithm

M_i = total mass of i^{th} item

GLOSSARY OF SYMBOLS (continued)

n_i = modal density of i^{th} item

NR = noise reduction

R_i = real part of Z_i

S_p = pressure spectral density

t = structural thickness

TL = transmission loss

y_i = complex displacement amplitude of i^{th} item

Z_i = mechanical impedance (flexural or torsional of i^{th} item

η_i = inertial loss factor of i^{th} item

η_{ij} = coupling loss factor for energy flow from i^{th} to j^{th} item

θ = angle between mounting truss and spacecraft axis

κ_i = flexural radius of gyration of i^{th} item

$\kappa_{\phi,i}$ = polar radius of gyration for cross-section of i^{th} item

Π_{ij} = energy flow (power) from i^{th} to j^{th} item

GLOSSARY OF SYMBOLS (continued)

$\rho_{\ell}^{(i)}$ = lineal density of i^{th} item (where appropriate)

$\rho_{p}^{(i)}$ = material density of i^{th} item

$\rho_{s}^{(i)}$ = surface density of i^{th} item (where appropriate)

τ = torque

ω = radian frequency

Ω = angular velocity

INTRODUCTION

20129

This second quarterly report on Contract NAS5-9601 continues our discussion of sound and vibration transmission in a model of the OGO spacecraft-shroud system. The basic formulas and concepts that are used to predict sound transmission were developed in the first quarterly report. In the present report, we continue the development with a calculation of spacecraft-to-shroud vibration ratios for mechanically transmitted energy. A calculation of the noise reduction of the fiberglass shroud is also included.

An experimental study of acoustical and vibrational energy transfer in the OGO system should provide an extremely useful adjunct to theoretical analyses. In this report a series of experimental studies are outlined that are designed to test and to complement the theoretical calculations. As complete a series of experiments as possible is desirable so that most of the important structural and inter-structure coupling parameters could be determined completely from the experimental analysis. In this way, one does not have to rely on the theoretical estimates for prediction of energy transmission.

IV CALCULATIONS OF VIBRATION TRANSMISSION

In this section we calculate the ratio of mean square transverse velocity of spacecraft panels to the mean square transverse velocity of the ring frame and the spacecraft shroud. The structural configuration is generally similar to the actual OGO-shroud system, but the structural parameters are left fairly general in the development of the theory. When the vibration ratios are computed, parameters representative of the OGO spacecraft and its shroud are used. The mechanical elements that make up the model are shown in Fig. 1. The rectangular spacecraft is an open ended box at its top and bottom which sits on four mounting trusses that make an angle θ with the vehicle axis. These trusses attach to a ring frame that is mounted directly on the shroud. The shroud is exposed to the external sound field.

4,1 Spacecraft to shroud energy ratio

The four structural elements in Fig. 1, the shroud, ring frame, mounting truss, and spacecraft, form a connected set of multimodal systems of the type described in section 2.2 of Ref. 1. In order to calculate the energy ratio between the shroud and the spacecraft, we need to know the power input to each structural section, the internal loss factors, and the coupling loss factors between the connected structures. The

calculations can be simplified by making some assumptions that are not only appropriate to OGO, but very likely to most spacecraft configurations of this type.

The energy balance equation for the shroud is given in Eq. (3,2.3a) of Ref. 1. The power transmitted from the shroud into the ring frame has not been included in that equation. It is likely to be small compared to the power dissipated by the shroud in internal damping and compared to the power re-radiated by the shroud to the interior volume and back into the surrounding medium. We therefore assume that the energy level of the spacecraft shroud is not significantly affected by the attachment of the ring frame.

If the shroud energy E_2 is assumed to be known, then the unknowns are the ring frame, mounting truss, and spacecraft energies E_5, E_6, and E_4. The set of Eqs. (2,3.1) of Ref 1 becomes for the four structural elements of our model

$$(n=5) \quad 0 = \eta_{56} n_5 \left(\frac{E_5}{n_5} - \frac{E_6}{n_6}\right) - \eta_{52} n_5 \left(\frac{E_2}{n_2} - \frac{E_5}{n_5}\right) + \eta_5 E_5$$

$$(n=6) \quad 0 = \eta_{64} n_6 \left(\frac{E_6}{n_6} - \frac{E_4}{n_4}\right) - \eta_{65} n_6 \left(\frac{E_5}{n_5} - \frac{E_6}{n_6}\right) + \eta_6 E_6 \qquad (4,1.1)$$

$$(n=4) \quad 0 = -\eta_{46} n_4 \left(\frac{E_6}{n_6} - \frac{E_4}{n_4}\right) + \eta_4 E_4$$

In writing these equations we have used the symmetry relation Eq (3,2.4) in Ref. 1.

We note that in the first of the Eqs. (4,1.1) that if the ring frame to shroud coupling loss factor η_{52} exceeds its coupling loss factor to the mounting truss η_{56} and its internal loss factor η_5, then modal energy equilibrium will exist between the shroud and the ring frame, i.e.,

$$\frac{E_2}{n_2} \simeq \frac{E_5}{n_5} \qquad \text{if } \eta_{52} \gg \eta_{56}, \eta_5. \qquad (4,1.2)$$

Since the ring frame is intimately attached along its full length to the spacecraft shroud, we can presume that its energy coupling to the shroud will be large. The result of this intimate attachment between the shroud and ring frame results in the elimination of the first of the Eqs. (4,1.1) and its replacement with (4,1.2).

With these assumptions, we have a three element structure of the kind that has been studied previously.[2] Using the second and third equations in Eq. (4,1.1) we can derive an expression for the ratio of spacecraft to ring frame energy in a frequency band. The result is

$$E_4/E_5 = \eta_{56}\eta_{64} \left[(\eta_6+\eta_{65}+\eta_{64})\ (\eta_4+\eta_{46}) - \eta_{64}\eta_{46}\right]^{-1} \qquad (4,1.3)$$

where η_{56} is the ring frame to mounting truss coupling loss factor,

η_{64} is the mounting truss to spacecraft coupling loss factor, and

η_4, η_6 are the spacecraft and mounting truss dissipative loss factors, respectively.

If the mounting truss of the OGO structure has very light damping and is well coupled to the ring frame and the spacecraft, then we can assume

$$\eta_6 \ll \eta_{65} + \eta_{64} \quad .$$

In this event, Eq. (4,1.3) simplifies to

$$E_4/E_5 \simeq \eta_{56}\eta_{64}(\eta_4\eta_{65} + \eta_4\eta_{64} + \eta_{65}\eta_{46})^{-1} \quad . \qquad (4,1.4)$$

Expressions for the coupling loss factors in terms of the flexural and torsional impedances of the structural attachments are developed in the following sections.

4,2 Coupling loss factor calculations

Our next task is to evaluate the structural loss factors that appear in Eq. (4,1.3) either on the basis of theoretical analysis or by an appeal to experiment. The internal loss factors η_4 and η_6 that describe the dissipation in the spacecraft and the mounting truss must at the present time be experimentally determined. Some recent gains have been made in the estimation of internal damping of structures,[3] but they are not sufficiently advanced so that we can confidently use these estimates for engineering predictions.

The coupling loss factor is computed from its defining formula,

$$\eta_{ab} \equiv \Pi_{ab}/\omega E_a \quad . \tag{4,2.1}$$

The average energy E_a is quadratically dependent on the standing wave amplitudes in subsystem (a). The power flowing from (a) to (b), Π_{ab} also depends quadratically on these amplitudes and on the force and moment impedances of the connected structures at their attachment points. In a linear system, the ratio of power to stored energy will therefore be independent of the wave amplitudes and will depend on geometrical and physical parameters of the attached structures.

Computation of η_{56}. Due to the way the ring frame is attached to the shroud, flexural motion of the ring frame (5) will only have displacements normal to the shroud (2). Let this displacement have a complex amplitude y_5. Then for vibrations at frequency ω and sinusoidal spatial dependence, the flexural energy of the ring frame is

$$E_5 = \frac{1}{4} M_5 \omega^2 |y_5|^2 \quad . \tag{4,2.2}$$

The internal impedance that the ring frame has as a source of excitation for the mounting truss is the ratio of moment to angular velocity parallel to the spacecraft axis at the point of its attachment to the mounting truss. In terms of the ring frame parameters, assuming $e^{-i\omega t}$ time dependence,[4]

$$Z_5 = 2(1-i)\rho_\ell^{(5)}\kappa_5^2 c_5^2 \, c_F^{(5)^{-1}} \qquad (4,2.3)$$

where ρ_ℓ, κ, c, and c_F are the lineal density, radius of gyration, longitudinal wavespeed, and bending wavespeed of the ring frame.

Ring frame flexure will excite both torsional and flexural waves in the mounting truss. The ratio of moment to angular velocity for a free torsional wave in the mounting truss is[5]

$$Z_6^T = \rho_\ell^{(6)}\kappa_\phi^{(6)} \, c_T^{(6)} \qquad (4,2.4)$$

where κ_ϕ is the polar radius of gyration of the mounting truss cross-section and $c_T = c_s\sqrt{K/J}$, is the torsional wavespeed. In the definition of c_T, the shear wavespeed in the material is c_s, and J and K are inertial and stiffness constants for torsional motion. The mounting truss flexural impedance is taken to be the ratio of moment applied to a pinned end of a semi-infinite beam to the resulting angular velocity[6]

$$Z_6^F = (1-i)\rho_\ell^{(6)}\kappa_6^2 c_6^2 \, c_F^{(6)^{-1}} \qquad (4,2.5)$$

The total "load" impedance that the mounting truss presents to the ring frame at the attachment point will now be derived. The junction between the ring frame and mounting truss is reconstructed in Fig. 2. The ring frame is replaced by an infinite beam constrained to have flexural displacements in

the x_2 direction only and the mounting truss is a semi-infinite beam which attaches to the ring frame. The junction is the origin of the coordinate system. The direction x_3 is the vehicle axis. We have noted previously[7] that the spacecraft is softest to a torsion in that direction. Such a torsion will result from both torsional waves in the mounting truss, and flexural waves in the mounting truss with displacements parallel to x_1. Both of these motions are generated by a flexure of the ring frame.

Torsional waves in the ring frame will generate flexural displacements in the (x_2, x_3) plane which will not produce axial torsion on the spacecraft. We therefore neglect this component of ring frame motion and only consider the loading that the mounting truss produces for ring frame flexure.

Let the angular velocities due to mounting truss torsion and flexure at the junction be Ω_T and Ω_F as shown in Fig. 2. Since the ring frame will not allow angular velocity in the x_2 direction at the junction, one must have

$$\Omega_F \cos\theta = \Omega_T \sin\theta \qquad (4,2.6)$$

The axial (or x_3) component of angular velocity at the junction is

$$\Omega_3 = \Omega_F \sin\theta + \Omega_T \cos\theta \qquad (4,2.7)$$

The reaction torque to this acial angular velocity at the junction is

$$\tau_3 = \tau_T \cos\theta + \tau_F \sin\theta \qquad (4,2.8)$$

where τ_T and τ_F are related to the appropriate angular velocities by the impedances (4,2.4) and (4,2.5). One has therefore,

$$\tau_3 = \Omega_T Z_T \cos\theta + \Omega_F Z_F \sin\theta \qquad (4,2.9)$$

We define the ratio of τ_3 to Ω_3 as the mounting truss load impedance Z_6:

$$Z_6 = (Z_6^F + Z_6^F \tan^2\theta)(1+\tan^2\theta)^{-1} \qquad (4,2.10)$$

One can see that the correct impedance is obtained in the limits of $\theta=0$ and $\theta=\pi/2$.

The power transferred from (5) to (6) can be expressed in terms of these impedances and the axial component of angular velocity of the ring frame at the junction, with the mounting truss detached:

$$|\Omega_5|^2 = \alpha^2 \, k_F^{(5)^2} \, |y_5|^2 \quad . \qquad (4,2.11)$$

The power transferred is then obtained from considering the equivalent circuit for the junction, Fig. 3:

$$\Pi_{56} = \frac{1}{2} |\Omega_5|^2 \left| \frac{Z_5}{Z_5 + Z_6} \right|^2 R_6 \ , \qquad (4,2.12)$$

where

$$R_6 \equiv \text{Re}\ (Z_6) \quad .$$

Placing (4,2.12) and (4,2.2) into (4,2.1) we get the desired result

$$\eta_{56} = \frac{2k_F^{(5)2}}{\alpha M_5} \left| \frac{Z_5}{Z_5 + Z_6} \right|^2 R_6 \quad . \qquad (4,2.13)$$

If (4,2.3) and (4,2.10) are used, all the quantities contained in (4,2.13) can be calculated from basic structural parameters.

Computation of η_{64}. The flexural and torsional waves generated in the mounting truss by the ring frame will reverberate on the truss and have their amplitudes built up until the power input from the frame equals the power transmitted back into the ring frame and on into the spacecraft. The torsional and flexural wave amplitudes incident on the truss-spacecraft junction are therefore not equal to those directly generated at the truss-frame junction.

If the displacement amplitude in the flexural truss motion is y_6, then the flexural energy in the truss is

$$E_6^F = \frac{1}{4} M_6 \ ^2 |y_6|^2 \quad , \qquad (4,2.14)$$

Again assuming sinusoidal spatial dependence, if the angular velocity amplitude associated with the torsional wave is Ω_6^T, then the torsional energy is

$$E_6^T = \frac{1}{4} M_6 \kappa_{\phi,6}^2 |\Omega_6^T|^2 \quad . \tag{4,2.15}$$

If equilibrium has been achieved between torsional and flexural modes of the mounting truss, we require

$$E_6^F/n_6^F = E_6^T/n_6^T \quad , \tag{4,2.16}$$

where n_6^F and n_6^T are modal densities for flexural and torsional modes at the mounting truss. The total energy of the truss is

$$E_6 = E_6^F + E_6^T = E_6^F \, (1+n_6^T/n_6^F) \quad . \tag{4,2.17}$$

At the junction between the mounting truss and the spacecraft, the source impedance for the axial torsion is Z_6 and the load impedance is Z_4. The impedance Z_4 is taken to be that of a plate edge for a normal moment. This impedance has been computed by Eichler. His expression is

$$Z_4 = \rho_s^{(4)} \kappa_4 c_4 \, (A-iB)/(A^2B^2) \, k_F^{(4)2} \tag{4,2.18}$$

where

$$A = 0.189$$
$$B = 0.275 \, \ell n(k_F^{(4)} w/2.5) \quad . \tag{4,2.19}$$

Here, $\rho_s^{(4)}$ is the surface density, κ_4 is the flexural radius of gyration, c_4 is the material longitudinal wavespeed, and $k_F^{(4)}$ is the flexural wavenumber. The half-width of the ring frame is w. The power transferred is

$$\Pi_{64} = \frac{1}{2} |\Omega_6|^2 \left| \frac{Z_6}{Z_6 + Z_4} \right|^2 R_4 , \qquad (4,2.20)$$

where Ω_6 is the total axial component of the truss angular velocity when it is pinned at the junction but the spacecraft is absent. The axial component of flexural angular velocity is $\kappa_f^{(6)} \omega y_6 \sin\theta$ and the axial component of torsional angular velocity is $\Omega_6^T \cos\theta$. The total mean square axial angular velocity is therefore

$$\frac{1}{2} |\Omega_6|^2 = \frac{1}{2} k_f^{(6)2} \omega^2 |y_6|^2 \sin^2\theta + \frac{1}{2} |\Omega_6^T|^2 \cos^2\theta \qquad (4,2.21)$$

Placing (4,2.21) in (4,2.20) and using (4,2.20) and (4,2.17) to define η_{64}, we arrive at

$$\eta_{64} = 2 \frac{k_f^{(6)2} R_4}{\omega M_6} \left| \frac{Z_6}{Z_6 + Z_4} \right|^2 \frac{\sin^2\theta + \frac{n_6^T}{n_6^F} \frac{\cos^2\theta}{k_f^{(6)2} \kappa_{\phi,6}^2}}{1 + n_6^T/n_6^F} \qquad (4,2.22)$$

The calculations for the coupling loss factors and energy ratios are clearly quite tedious and will depend on basic structural parameters in an involved way. Calculations of the energy ratios will require the use of a computer.

4,3 Computation of velocity ratios for the OGO model

In this section we shall use Eqs. (4,1.2) and (4,1.3) to predict the ring frame to shroud and spacecraft to ring frame energy and vibration amplitude ratios. A multiplication of these ratios will provide the ratio of spacecraft to shroud vibration levels.

Structural parameters for the elements in Fig. 1 have been chosen by reference to engineering drawings of OGO provided by NASA. There has been some idealization of the geometry of these elements, but an attempt has been made to follow as closely as possible the original dimensions and configuration in our choice of parameters.

The exterior glass-reinforced-plastic (GRP) shroud was described in Chapter 3 of Ref. 1. It is a cylinder, 6 ft. in diameter, 11 ft. long, with a thickness of 0.1 ins. It has a density of 113 lbs per cubic foot, and a Young's modulus of 2.75×10^6 lbs per sq. in. In cgs units these parameters are

$$t_2 = 0.25 \text{ cm} \qquad \rho_p^{(2)} = 1.8 \text{ gm/cm}^3$$
$$A_2 = 6.1 \times 10^4 \text{ cm}^2 \qquad c_2 = 3.4 \times 10^5 \text{ cm/sec} \tag{4,3.1}$$

The ring frame is also modeled on the basis of prints supplied by NASA. It is an aluminum channel beam having the dimensions shown in Fig. 4. Allowed motion of the ring frame consist of torsion along its axis and flexure normal to the shroud. The dimensions are shown in the figure. We see from Eqs. (4,2.2) (4,2.3) and (4,2.11) that the required parameters are ring frame mass M_5, flexural radius of gyration κ_5, lineal density $\rho_\ell^{(5)}$, and flexural wavespeed $c_F^{(5)}$. Since there are four mounting trusses, we consider the structural system to be divided into four equal and parallel portions. Our calculations throughout will treat the system as though it were divided into four parallel sections.

In terms of the dimensions in Fig. 4, the flexural radius of gyration is given by

$$\kappa_5^2 = \frac{w(y-t/2)^2+(x^3+y^3)/3}{a+w} \qquad (4,3.2)$$

where

$$x = a-y; \qquad y = (a^2+wt)/2(a+w) \; . \qquad (4,3.3)$$

These results are obtained from the definition of the flexural radius of gyration as the second moment of the cross-sectional area about the neutral axis of the beam. The flexural wavespeed on the ring frame is given by

$$c_F^{(5)} = (\omega\kappa_5 c_5)^{1/2} \qquad (4,3.4)$$

and the flexural wavenumber is defined by

$$k_F^{(5)} = \omega / c_F^{(5)} \quad .$$

Equations (4,3.2) and (4,2.4) along with the dimensions in Fig. 4 provide sufficient information for the evaluation of the structural dynamics of the ring frame.

The mounting truss for the OGO spacecraft is a double beam (wishbone) connection between the corner of the spacecraft and the mounting truss. We have simplified and idealized this in the model design as a single channel beam of dimensions and configuration shown in Fig. 5. The single channel beam is designed to have the same torsional rigidity and total mass as the two beams that it replaces. As mentioned previously, it has two modes of motion that are effective in transmitting energy to the spacecraft. They are flexure in the direction indicated in the sectional view of Fig. 5 and torsion along the axis of the mounting truss.

From Eqs. (4,2.4) and (4,2.5) it is necessary that we evaluate the lineal density $\rho_\ell^{(6)}$, the polar radius of gyration for the channel cross section $\kappa_{\phi,6}$, the torsional wavespeed $c_T^{(6)}$, the flexural radius of gyration for the power-transmitting component of flexure, and the flexural wavespeed for this mode of motion $c_F^{(6)}$. The lineal density can be obtained from the cross sectional area of the beam shown in Fig. 5 and the volume density of the material

(aluminum) from which the beam is constructed. The flexural radius of gyration for mounting truss flexure is given by

$$\kappa_6^2 = \frac{\frac{1}{3} w^3 + a(w+t/2)^2}{a + w} \qquad (4,3.5)$$

where a and w are taken from Fig. 5 and have the same geometric significance (but not the same value) as indicated in Fig. 4. The polar radius of gyration κ_ϕ is found finding the sum of the squares of the radii of gyration in the two principle directions of the channel. This amounts to a summation of the forms in Eq. (4,3.2) and (4,3.5). The flexural wavespeed for the ring frame is given by

$$c_F^{(6)} = (\omega \kappa_6 c_6)^{1/2} \qquad (4,3.6)$$

The longitudinal wavespeed for the channel beam is the same as it was for the ring frame, i,e, $c_6 = c_5$. The angle that the mounting truss makes with the axis of the spacecraft is 0.44 radians or approximately 25^o.

In Fig. 6, we show the configuration of the spacecraft relative to the mounting trusses that support it. As noted previously, a certain section of the spacecraft is assigned to each of the four mounting trusses and the assumption is that there is no average interchange of energy between these sectors. The panels of the spacecraft box are made up of the orthotropic sandwich material indicated in the section diagram. As we see from Eq. (4,2.22), the input impedance

to torsional excitation along the vertical edges of the spacecraft box is needed. Unfortunately, the only calculation of torsional edge admittance of plate that exists is Eichler's isotropic plate analysis[9]

In order that we may apply Eichler's results to this problem, we have decided to model the spacecraft panels by an equivalent isotropic sandwich structure. This equivalent panel has a bending rigidity that is the geometric mean of the bending rigidities of the actual panel construction in the two principle directions. The resulting panel is a sandwich of 1.8 cm thickness with two aluminum skin facings of .052 cm each. The overall dimensions of the spacecraft are not altered. The Young's modulus of the material from which this sandwich is constructed would have to be roughly 6% less than that of aluminum. This difference is assumed to be negligible and has not been taken into account in the computations.

We can see from Eqs. (4,2.18) and (4,2.19) that we need parameters the surface density of the spacecraft panels $\rho_s^{(4)}$ which is obtainable from the section diagram in Fig. 6, and the radius of gyration for flexural waves on the panel κ_4, given by

$$\kappa_4 = H_4/2 \ . \qquad (4,3.7)$$

The longitudinal wavespeed of the material c_4 is that of aluminum and hence $c_4=c_5=c_6$ and $k_F^{(4)}$, the flexural wavenumber for panel waves, is given by

$$k_F^{(4)} = \omega/c_F^{(4)} = (\omega/\kappa_4 c_4)^{1/2} \quad . \qquad (4,3.8)$$

The parameter remaining in Eq. (2,2.22) is the ratio of modal density for torsional and flexural motions in the ring frame which is given by[2]

$$n_6^T/n_6^F = 2c_F^{(6)}/c_T^{(6)} \quad . \qquad (4,3.9)$$

Applying these structural parameters in Eq. (4,2.13), we can obtain the ring frame to mounting truss coupling loss factor η_{56}. The result of this calculation is shown in Fig. 7. We have plotted η_{56} on a logarithmic scale against a logarithmic frequency scale, where the frequencies shown are octave band center frequencies. The rate of decrease with frequency very close to 1.5 db per octave, corresponding to a frequency dependence of $f^{-1/2}$.

The coupling loss factor for ring frame to spacecraft power transfer, η_{64} has also been calculated. The results of the computation are also shown in Fig. 7. We note that extrodinarily large values of coupling loss factors at low frequencies are obtained. These indicate that quite intimate coupling between the mounting truss and the spacecraft exists for these frequencies. Complete energy equilibrium between these two structures at these frequencies, perhaps up to a frequency of the order of 500 cps should be expected.

The ratio of spacecraft to ring frame energy in any frequency band is given in Eq. (4,1.3). The loss factors η_{65} and η_{46} will be obtained from the known loss factors η_{56} and η_{64} respectively by use of the symmetry relation Eq. (3,2.4) in Ref. 1. One has therefore

$$\eta_{65} = \frac{n_5}{n_6}\,\eta_{56}; \qquad \eta_{46} = \frac{n_6}{n_4}\,\eta_{64} \tag{4,3.10}$$

where the modal density ratios are given by

$$\frac{n_5}{n_6} = \frac{L_5}{L_6}\,\frac{c_F^{(6)}}{c_F^{(5)}}\left(1+2\,\frac{c_F^{(6)}}{c_F^{(6)}}\right)^{-1} \tag{4,3.11}$$

$$\frac{n_6}{n_4} = \frac{8\kappa_4 c_4 L_3}{A_4 c_F^{(6)}}\left(1+2\,\frac{c_F^{(6)}}{c_T^{(6)}}\right) \tag{4,3.12}$$

In these equations the length of a mounting truss is L_6 and L_5 is 1/4 of the total length of the ring frame. The total area of the spacecraft box is A_4. The remaining parameters have been defined previously. The relation between the (space-time) mean square velocity response and the average energy is $E = Mv^2$. Thus, the ratio of mean square velocity of the spacecraft to mean square transverse velocity of the ring frame is given by

$$\frac{v_4^2}{v_5^2} = \frac{E_4}{E_5}\frac{M_5}{M_4} \qquad (4,3.13)$$

This ratio has been computed for the structural parameters of the model and is displayed in Fig. 8. We see that above 100 cps the spacecraft vibrates approximately 13 db less than the ring frame. We have also used Eq. (4,1.2) to obtain the ring frame to shroud vibration ratios. The ratio of ring frame to shroud modal density is

$$\frac{n_5}{n_2} = 2\frac{L_5\kappa_2 c_2}{c_F^{(5)} A_2} \quad . \qquad (4,3.14)$$

The velocity ratio is also displayed in Fig. 8. We note that the ring frame velocity decreases as the frequency increases at a rate of approximately 1.5 db per octave, in direct consequence of the difference in modal density between the one dimensional ring frame and the two dimensional shroud modal densities. If this velocity ratio is expressed logarithmically, the net ratio of spacecraft to shroud velocity response amplitude ranges from approximately 27 to 35 db over the frequency range of interest. It is this vibration ratio that we wish to compare with that derived for the acoustic transmission path.

V. ACOUSTIC NOISE REDUCTION BY THE SHROUD

The elements of the acoustic transmission path consist of an exterior sound field, a spacecraft enclosing shroud, an interior acoustic space, and the spacecraft. In Chapter 3 of Ref. 1 idealized models of these elements and our approach toward predicting vibration levels due to acoustic excitation for our model of the spacecraft are described. We have continued with this approach and relevant progress on the shroud noise reduction is reported herein.

In Ref. 1, a set of equations was developed to predict the flow of acoustic energy into resonant vibration of the shroud, the flow of energy from the shroud into the interior acoustic space, and finally the flow of energy into the spacecraft. (See 3,2). This set of equations can be solved for the relative vibration and sound pressure levels of each element of the acoustic path in terms of the exterior sound pressure level, the modal densities, and coupling and internal loss factors of the elements. A method for predicting the coupling loss factor between a diffuse sound field and a cylindrical shroud was developed.

5,1 Introduction to noise reduction

In this chapter we focus our attention on a preliminary step toward the prediction of spacecraft vibration levels: the prediction of the noise reduction, NR, due to the shroud. The noise reduction is defined as the difference in sound pressure levels (expressed in dB) outside and inside the shell. References 10 and 11 give a detailed discussion of noise reduction problems and much of the analysis in this paper is based on work contained in these references.

The noise reduction of the shell can be conveniently studied in three regions of frequency:[2] low frequencies below the first resonant frequencies of the shell and the interior acoustic space; intermediate frequencies at which either the shell or the interior space vibrates resonantly; and high frequencies at which both elements vibrate resonantly. We restrict our attention in this report to high frequencies. When the shell dimensions exceed both the acoustic and flexural wavelengths, its response to a sound field may be thought of as composed of two forms of motion. First, the sound wave will induce a motion in the shell matching it in frequency and trace wavelength. Between the ring frequency and the critical frequency, the induced wavelength will always exceed the "natural" bending wavelength for the shell (i.e. there will be no AF modes), and the shell response will be that of a limp wall. This mass-controlled response we refer to as the "forced wave", "forced", or "nonresonant" response.

At the boundaries of the shell, the forced wave alone will not satisfy the boundary conditions. In order to do so, bending motions, which are solutions of the homogeneous wave equation, are generated that must combine with the forced waves to satisfy the boundary conditions. These additional motions we refer to as the "free wave", "free", or "resonant" response. All the motion is "forced", of course, in the sense that there would be no response without excitation, but the breakdown of the response into this division is a convenient one.

At and below the ring frequency, the induced wavelength of the forced wave response can match the "natural" wavelength of one of the shell modes. At these frequencies the

division of response into "forced" and "free" wave response is no longer simple and may not be convenient. A similar statement can be made for frequencies above the critical frequency.

5,2 Noise reduction for resonant shroud vibrations

At frequencies above the critical frequency or below the ring frequency the sound power radiated into the interior acoustic space is controlled by the "free" resonant response of the shroud. Thus, we can use the power balance Eq's. (3,2.5) of Ref. 1 to predict the NR,

$$\underline{n}\underline{\eta}\underline{\varepsilon}_R = \underline{\varepsilon}_E \quad , \qquad (5,2.1)$$

where the underscore signifies a matrix. The modal density matrix $\underline{n}$, the coupling loss factor matrix, $\underline{\eta}$, and the modal energy matrices, $\underline{\varepsilon}_R$ and $\underline{\varepsilon}_E$, are defined on page 24 of Ref. 1. Using eq. (5,2.1), the ratio of the exterior pressure spectrum to the interior spectrum is

$$\frac{S_p^{(1)}}{S_p^{(3)}} = 1 + \frac{\eta_2}{\eta_{21}} + \frac{1}{n_2\eta_{21}}\left[2 + \frac{n_2}{\eta_{21}}\right]\left[\eta_3 + \frac{\eta_4\eta_{34}}{\eta_{43} + \eta_4}\right]. \qquad (5,2.2)$$

The NR follows by definition

$$NR \equiv 10 \log \left[\frac{S_p^{(1)}}{S_p^{(3)}} \right] . \qquad (5,2.3)$$

In Eq. (5,2.2) the quantity in brackets,

$$\eta_{loss} = \eta_3 + \frac{\eta_4 \eta_{34}}{\eta_{43} + \eta_4} , \qquad (5,2.4)$$

is obtained from the losses due to dissipation in the acoustic space and the spacecraft. In this report we will obtain the NR for several assumed values of η_{loss}. The shroud internal loss factor, η_2, cannot be calculated theoretically. However, past experience has shown that assumed values of $\eta_2 = 10^{-2}$ or 1/f can provide reasonable results. We will calculate the NR for both of these values. The remaining constants, η_{21}, n_2, and n_3 have been predicted in Ref. 1. The "free wave" NR for our model of the shroud is plotted as a function of frequency in Fig. 1 and is compared with the mass-law NR which will be calculated in the next section.

5,3 Noise reduction for nonresonant shroud vibrations

Between the ring frequency and the critical frequency, the coupling loss factor between the acoustic field and resonant vibrations of the cylindrical shroud is very small. Thus, in spite of large amplitude resonant vibrations in the shroud the sound power radiated into the interior at these frequencies is small. The forced vibrations, on the other hand, are strongly coupled to the acoustic field and in spite of their small amplitudes, they can radiate significant amounts of power into the interior. The actual NR can never

exceed either the forced-wave value or that calculated assuming free waves alone, since both forced and free motions exist on the shroud at all times.

To calculate the NR due to forced vibrations we follow the procedure used in reference 1. This procedure involves the transmission coefficient τ, defined as the ratio of the incident acoustic intensity to the transmitted acoustic intensity for an infinite panel. The transmission loss (TL) is defined by

$$TL \equiv 10 \log \left(\frac{1}{\tau}\right) \qquad (5,3.1)$$

Below the critical frequency, the sound transmission coefficient of an infinite panel is[12]

$$\tau(\phi) = \left[1 + \left(\frac{|Z_s| \cos\phi}{2\rho_o c_o}\right)^2\right]^{-1} \qquad (5,3.2)$$

where ϕ is the angle of incidence of the incoming acoustic wave, $|Z_s|$ is the magnitude of the complex ratio of the pressure difference on the two sides of the panel to the velocity of the panel perpendicular to its surface, and $\rho_o c_o$ is the characteristic acoustic impedance of the fluid medium. When the panel response is mass-controlled, the impedance magnitude can be expressed as

$$|Z_s| = \omega \rho_s \qquad (5,3.3)$$

where ρ_s is the panel mass per unit area. When the incident acoustic waves are distributed over all angles of incidence, the transmitted power is given by an average of τ over all angles of incidence (2π steradians):

$$I_{trans} = I_{inc}\,\bar{\tau} \qquad (5,3.4)$$

where

$$\bar{\tau} = \frac{\int_0^{\pi/2} \tau \cos\phi \sin\phi \, d\phi}{\int_0^{\pi/2} \cos\phi \sin\phi \, d\phi} \qquad (5,3.5)$$

Combining Eqs. (5,3.1-5) gives an expression for TL,[13]

$$TL = 20 \log\left[\frac{\omega\rho_s}{2\rho_o c_o}\right] - 10 \log_{10}\left[2.3 \log\left(1 + \frac{\omega^2\rho_s^2}{4\rho_o^2 c_o^2}\right)\right] \qquad (5,3.6)$$

Eq. (5,3.6) is valid for an infinite panel which is responding in a mass-controlled manner. However, when the dimensions of a finite panel are large compared to the acoustic wavelength this equation is also valid for predicting the TL resulting from the forced response of the finite panel.

To calculate the NR we find the spectral level of intensity incident on the shroud from a diffuse acoustic field. This is given in terms of the pressure spectrum by

$$S_{I_{inc}} = \frac{S_p}{4\rho_o c_o} \qquad (5,3.7)$$

The net spectral power transmitted into the interior acoustic space from the external diffuse field is

$$\Pi_{13} = \frac{\tau A_2}{4\rho_o c_o}\left[S_p^{(1)} - S_p^{(3)}\right] \quad , \qquad (5,3.8)$$

where A_2 is the surface area of the shroud. This power must be equal to that dissipated inside the shroud. Since the interior sound field is resonant, the dissipated power can be expressed in the statistical energy forms developed in Ref. 1;

$$\Pi_{diss} = \omega \eta_{loss} n_3 e_3 \qquad (5,3.9)$$

where η_{loss} is defined in Eq. (5,2.4). The modal energy of the acoustic space e_3 is given by

$$e_3 = V_3 S_p^{(3)} / \rho_o c_o^2 n_3 \ . \qquad (5,3.10)$$

Equating Eqs. (5,3.8) and (5,3.9) gives

$$NR = 10 \log_{10}\left[1 + \frac{4\omega V_3 \eta_{loss}}{\tau A_2 c_o}\right] \qquad (5,3.11)$$

where V_3 is the volume of the interior acoustic space, and A_2 is the surface area of the shroud.

The NR due to forced vibrations given by Eq. (5,3.11) is plotted in Fig. 1 for several values of $4\omega V_3 \eta_{loss}/A_2 c_o$ and is compared with the NR due to resonant vibrations. Note that the overall NR is controlled by forced vibrations for frequencies between the ring frequency and the critical frequency, and varies from near zero to around 20 db.

5,4 Directions of future study

During the next quarter we will concentrate on the acoustic acceptance properties of the spacecraft model. This work will complete the analysis of the acoustic path.

VI. EXPERIMENTAL ANALYSIS OF RANDOM LOAD TRANSMISSION IN A SPACECRAFT

One of our responsibilities under contract NAS5-9601 is the design of a series of experiments of sound and vibration transmission in a model of the OGO spacecraft. In this chapter we present some general guidelines and considerations for the design of specific experiments. The designs for particular experiments are not included in the chapter.

6,1 Introduction

Experiments on structural configurations exposed to random acoustic environments can be and are carried on for a wide variety of purposes. The field of environmental testing includes experiments that are designed to "proof test" a structure. In such tests, the structure is subjected to an anticipated environment and one determines whether or not its structural integrity and/or its operational behavior are affected by the environment. Tests may also be run at lower levels of excitation to determine anticipated response at locations where sensitive equipment may be mounted. Vibration and acoustic specifications may be generated for particular equipments by such tests. The tests that we will propose for the OGO model do not include the former type of test at all but have elements in common with the latter.

A second major class of experiments is designed to merely gather data on structural and acoustic parameters. These parameters are usually obtained, either because they cannot be directly or conveniently calculated or because there is some wish to correlate a calculation with an experimental study. The experiments may be designed to gather only a

few bits of structural information or they may be designed to define almost all of the major parameters of the system. In either case the result of the experiment is a list of data that is to be used in theoretical analyses for the prediction of some other more complex bit of information about structural behavior. The types of experiments we describe here fall within this category. In fact, we propose measurements of many structural parameters that can be calculated from theoretical notions. In this way, predictions of vibration and load transmission can be based upon as much experimentally derived information as possible.

Finally of course there are experiments that one might call "research tests". Such experiments are used to directly test theoretical calculations of modal density, response ratios, damping, or other parameters. They may also be used to test theoretical assumptions about the way that the structure is behaving in various segments, frequency ranges, or modes of motion. Some of the experiments that we will propose fall in this category.

The spacecraft model to be analyzed is shown in Fig. 1. The detailed structure of this model is shown further in Figures 4, 5 and 6 and was discussed in the text of chapter 4. It should be designed to be as flexible in use as possible, i.e. it should be readily dismantled, and the addition of structural damping and acoustic absorption should be relatively simple. We do not feel that there are any conflicts between these requirements and the fundamental necessity for the model to be representable by the dynamical considerations outlined in chapters 4 and 5.

In the more detailed discussions to follow, the mechanical and acoustical paths are treated separately as they are

in the theoretical analyses. For each of the major acoustical and structural elements of each path we will describe those parameters that are most important in establishing the energy transfer and storage. We will also try to give some indication of the problems and possibilities for the experimental determination of each important parameter. We will describe various energy transmission experiments. It may be desirable to perform these on various segments of the energy transmission chain. Experiments on transmission of energy in the vibrational and acoustical chains separately or together should also be carried out. Based on this very detailed breakdown, a fairly high degree of flexibility in the spacecraft model construction is desirable. This flexibility would not in general be available to us if we were studying an actual spacecraft. The essential difference is not in the complexity of the system, but in the degree of ease with which one can dismantle various segments of the system and then reconnect them and have the structure remain in its initial state.

In the remaining sections of this chapter we shall describe the primary parameters of the structural elements that are amenable to experimental investigation and are important to the noise and vibration transmission. The mechanical path and the acoustical path will be discussed separately. For each path we may wish to study modal density, damping, coupling, loss factors, noise and vibration ratios, etc. The energy transmission will be studied both for segments of the structures and for the major assembled sections of the model. This will be done both with and without simultaneous effects of acoustic and vibration transmission. Let us begin our discussion by

enumerating some of the experimental studies on the acoustical transmission path.

6,2 Experimental studies of the acoustical path

Item No. 1 in the acoustic transmission path is the exterior acoustic space and the sound field within it that excites the spacecraft shroud. Two major forms of the exterior sound field will be investigated. The simplest to generate experimentally and to correlate with analysis is the diffuse reverberant field. A diffuse sound field can be generated by exciting a large, reasonably "hard" acoustic space with a band of noise. Almost any large room is suitable for this purpose, provided that unusually large acoustic absorption (absorption coefficients greater than 30% say over major parts of the wall area) is not present. A non-diffuse directive sound field may also exist on the vehicle. This type of field can be applied to the vehicle surface by increasing the absorption in the room so that the "direct field" of the sound source extends out perhaps a distance of 10 - 15 ft. from the sound projector. If the shroud is placed in this field it will experience relatively more acoustic energy incident from some angles than from others. There are cases when this type of excitation may be more representative of the service environment of the vehicle than a purely diffuse sound field. A goal of our studies would be to test possible differences in the shroud mechanical response and in its sound transmission under these two types of incident sound fields.

It will be clear from the discussion in chapter 5 that it is fairly important to determine the relative amount of

sound transmitted through the shroud due to its forced wave (nonresonant) and resonant response. Since forced wave transmission is independent of structural damping, a way to find the relative importance of the two is to increase the shroud damping appreciably. Any increase in noise reduction must be due to the decrease in resonant transmission (except for the effects of added mass in the damping treatment, which should be included in the analysis of the results).

Theoretical evaluation of the resonant transmission involves the damping, modal density, and the radiation efficiency of the shroud. These parameters can be evaluated by mechanical and acoustic tests on the shroud structure. Damping may be measured by studies of decay rate in frequency bands. Modal density can be found at low frequencies by "counting peaks" of the resonant response as the existing frequency is altered. This is a useful technique until the bandwidth of individual resonant modes becomes comparable to the average frequency spacing between modes.

The radiation efficiency of the shroud can be found in several ways. Perhaps the most direct is to excite the shroud in frequency bands with a mechanical shaker. The radiated sound power can be computed from the sound level resulting in the surrounding room and from the acoustic absorption of the room. Random sampling of the mean square velocity over the surface of the shroud allows one to estimate its energy. The shroud to surrounding sound field coupling loss factor η_{21} is determined from Eq. (4,2.1). This coupling loss factor also determines the rate at which power will enter the shroud from a reverberant sound field

and the rate at which energy is radiated to the internal volume (item 3) by the resonant vibration of the shroud.

The resonant vibration of the shroud will probably exceed its forced wave response. As we have noted in chapter 5 and have implied in the discussion in the previous paragraph, it may or may not control the sound transmission. There is no question however that resonant motion will control the vibration levels of the ring frame. In cases where the possible failure of the shroud structure is of concern, the shroud acceleration levels and the associated strain levels at concentration points are also of interest. Shroud vibration levels as well as sound transmission measurements should be made with diffuse and directive sound fields incident on the shroud.

The important properties of the interior volume (item 3) for our study are its acoustical absorption and its geometry. The absorption of interior volume controls the sound pressure level when a fixed acoustical power is fed into this space. It is measured by making decay rate measurements of sound pressure in frequency bands, making allowance in the loss calculations for the sound that is transmitted outward through the shroud into the surrounding space.

The geometry will control the frequency location of the first few modes of the volume, and these may occur within the frequency range of interest. Geometry will also determine the "diffusion" of the sound field within. Diffusion can be measured by making microphone scans through the volume to see whether the sound pressure levels remain uniform on the average as one moves about the space. Strong

nonuniformities could result from excessive acoustic absorption in one part of the contained volume or perhaps a peculiar modal distribution. The existence of such effects are important in describing the acoustic environment of the spacecraft.

Finally, the acoustic and structural characteristics of the spacecraft box must be determined. These characteristics include the coupling loss factor between the spacecraft and the interior volume η_{43}, the structural damping, and the modal density. All these parameters can be measured in a manner similar to that described for the shroud. The coupling loss factor η_{43} is important for acoustical calculations, and the structural damping and modal density are parameters that apply equally well to the analysis of both acoustical and the vibrational paths.

Measurement of the spacecraft shroud NR is a study of the relative modal energy between the contained volume of the shroud and the exterior space. Further experiments on the acoustical path include placement of the spacecraft within the shroud using mechanical suspension that is extremely soft. In this way the complete acoustical chain from the exterior space to the spacecraft is represented and the resulting vibration levels on the spacecraft can be studied for comparison with the calculations. One may wish to alter various parts of the path by changing shroud damping or radiation efficiency (by removal of the ring frames) or by changing the directivity of the exterior sound field or by altering the acoustical absorption within the interior volume. In such a manner one could build up a fairly complete picture of the processes controlling the sound transmission path.

6,3 Experimental study of the mechanical path

The spacecraft shroud resonant vibration forms the random environment of the ring frame, item 5. In chapter 4 we assume that the coupling loss factor from the ring frame to the shroud would be much larger than the ring frame loss factor or its coupling loss factor to the mounting truss. It would be wise to test this hypothesis experimentally. This can be done by exciting the ring frame with bands of noise and observing its decay rate with the shroud heavily damped. The modal density for both torsional and flexural modes for the ring frame should also be measured both before and after it is attached to the shroud. With the shroud randomly excited, the flexural and torsional vibrational levels of the ring frame should be measured. The results of this experiment can then be correlated with the equal modal energy hypothesis made in chapter 4. The moment impedance of the ring frame, Z_5 describes the internal impedance of the ring frame as a source of energy for the mounting truss. This impedance should also be measured. Special impedance equipment would have to be obtained and/or developed for such measurements.

The important energy storage parameters of the mounting truss are the modal densities for torsional and flexural vibrations and the structural damping. It is also important to find the resonant frequencies of the first modes of vibration of the mounting truss, since only above this frequency will the truss act as a wave bearing system. The torsional and flexural wave impedances of the mounting truss channel beam should also be studied. The coupling loss factor to the ring frame may be measurable by decay rate techniques. This could be a difficult measurement. With

the mounting truss in place and the shroud excited, the ratio of mounting truss to ring frame and shroud response amplitudes should be monitored as a test of the calculations.

Finally the spacecraft should be studied as a recipient of vibrational energy from the mounting truss. Its modal density and damping will have been studied for the acoustic path. The moment impedance at the axial edges of the spacecraft box should be measured so that a comparison with Eichler's calculation can be made. The ratio of vibration levels of the spacecraft to the other mechanical elements in the vibration path can also be monitored and compared with theory. Special vibration control techniques may also be investigated. In order for the acoustic path not to interfere with mechanical measurements it may be necessary to take special precautions to reduce the acoustic transmission component to a very small value. One possibility would be to fill the space with a gas of very low characteristic impedance, such as helium. Another possibility is to reduce the interior volume reverberant sound levels by the addition of heavy acoustic absorption.

These brief discussions indicate the number and type of experiments that can be undertaken on the OGO model. They take full advantage of its flexibility and on the usefulness of being able to do fairly complete calculations on this system. We would strongly recommend that as many of these measurements as possible be carried out so that the most complete picture can be developed for the system. This is desirable because many of the concepts in predicting

the sound and vibration transmission in the OGO model are in their early stages of development. We feel that they give a good picture of the transmission processes in general, but there always will remain points that are difficult to resolve by theoretical analysis alone. The experience and techniques that would be developed by a set of experiments like those described here would be invaluable for further applications of the statistical energy method to the transmission of random loads in spacecraft.

NOTES AND REFERENCES

1. First Quarterly Report, Contract NAS5-9601, "Analytical Procedure for Determining Random Load Acting on a Spacecraft Due to a Primary Random Load Acting on an Exterior Structure," Bolt Beranek and Newman Inc., Cambridge, Massachusetts, 14 June - 31 August 1965, Chapter II.

2. R. H. Lyon and T. D. Scharton, "Vibrational Energy Transmission in a Three Element Structure," J. Acoust. Soc. Am., 38, 2, pp. 253-261, August 1965.

3. E. E. Ungar and J. R. Carbonell, "On Panel Vibration Damping Due to Structural Joints." Submitted for publication.

4. M. Heckl, "A Compendium of Impedance Formulas," BBN Report No. 774, Contract Nonr 2322(00), 26 May 1961, Eq. (VI-1).

5. E. E. Ungar, "Mechanical Vibrations," Chapter 6 of Mechanical Design and Systems Handbook (McGraw-Hill Book Company, Inc., New York 1964) p. 6-44.

6. Reference 4, Eq. VI-2

7. Monthly Progress Report No. 2, Contract NAS5-9601, "Analytical Procedure for Determining Random Load Acting on a Spacecraft Due to a Primary Random Load Acting on an Exterior Structure," Bolt Beranek and Newman Inc., Cambridge, Massachusetts, July 1 - 31, 1965

8. In reference 2, it was shown that this is a reasonable assumption.

9. E. Eichler, "Plate Edge Admittances," J. Acoust. Soc. Am., 36, 2, pp. 344-348, February 1964.

10. L. L. Beranek, Noise Reduction, McGraw-Hill Book Co., New York, 1960, Chapter 13.2.

11. R. H. Lyon, "Noise Reduction of Rectangular Enclosures with one Flexible Wall," J. Acoust. Soc. Am., 35, 11, 1791-97, 1963.

12. This equation, given in ref. 1, is credited to A. London, "Transmission of Reverberant Sound through Double Walls," J. Acoust. Soc. Am., 22, p. 270, 1950.

13. The TL is plotted in ref. 1, figure 13.7.

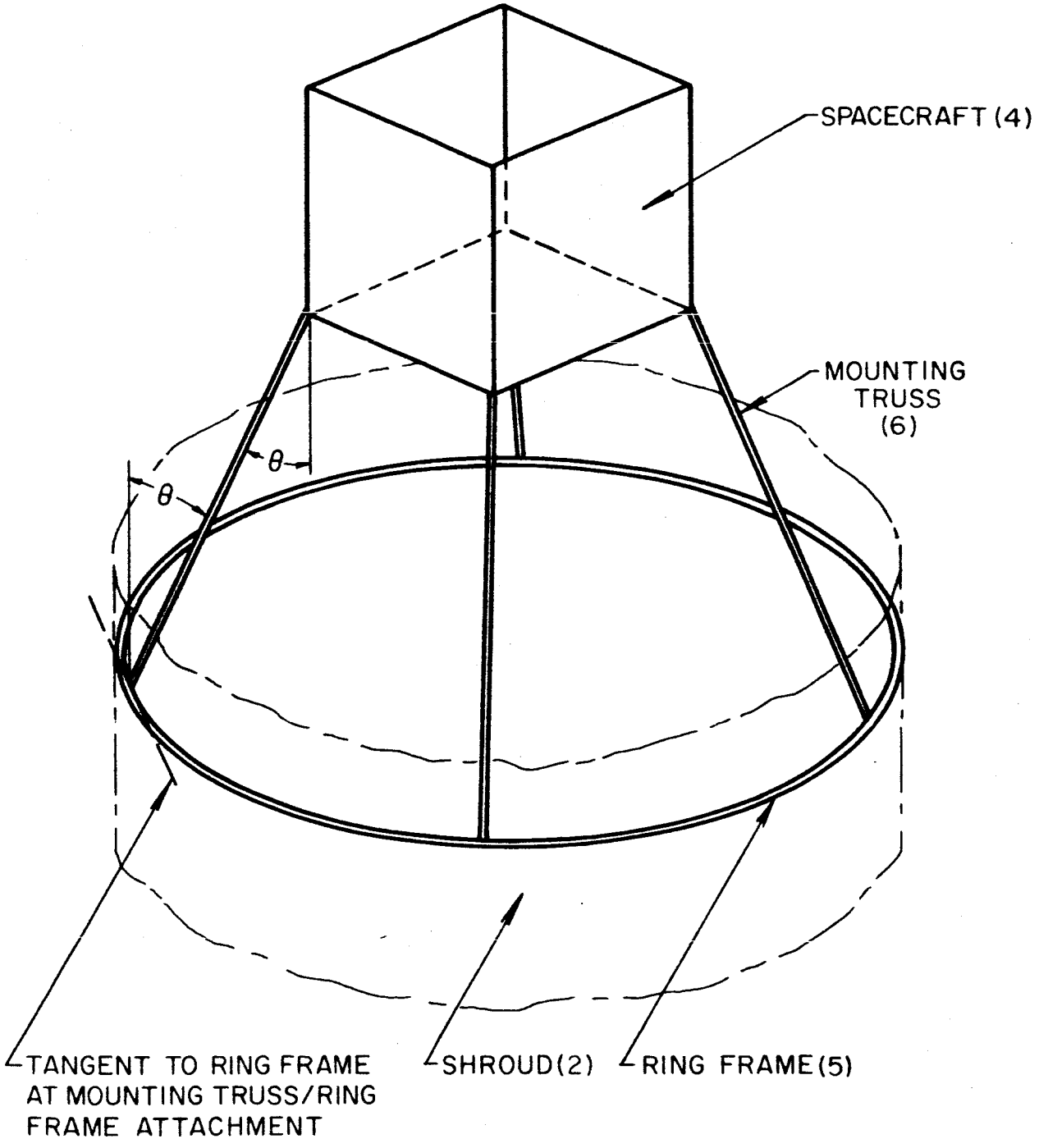

FIG. 1 SPACECRAFT CONNECTED TO RING FRAME BY THE MOUNTING TRUSS

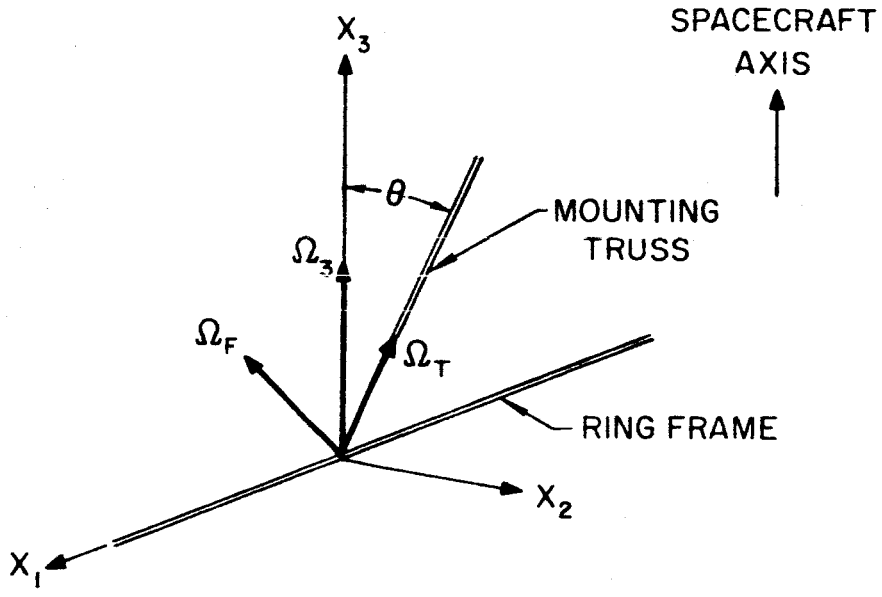

FIG. 2 GEOMETRY OF RING FRAME-MOUNTING TRUSS CONNECTION

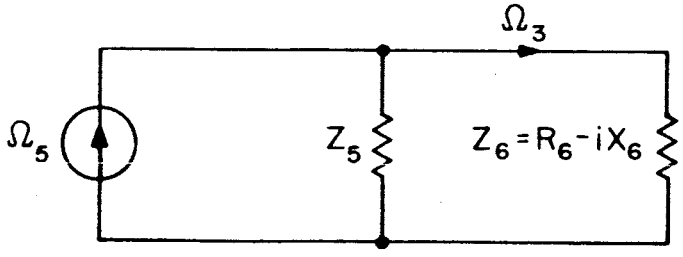

FIG. 3 EQUIVALENT CIRCUIT FOR DETERMINING POWER FLOW FROM RING FRAME TO MOUNTING TRUSS

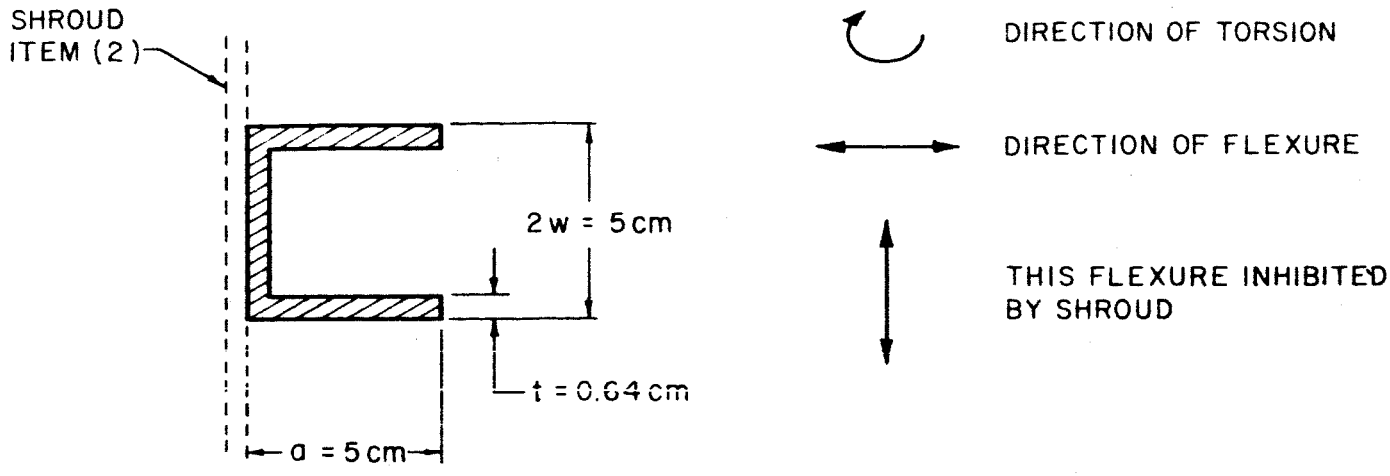

FIG. 4 CHANNEL BEAM MODEL OF RING FRAME, ITEM (5)

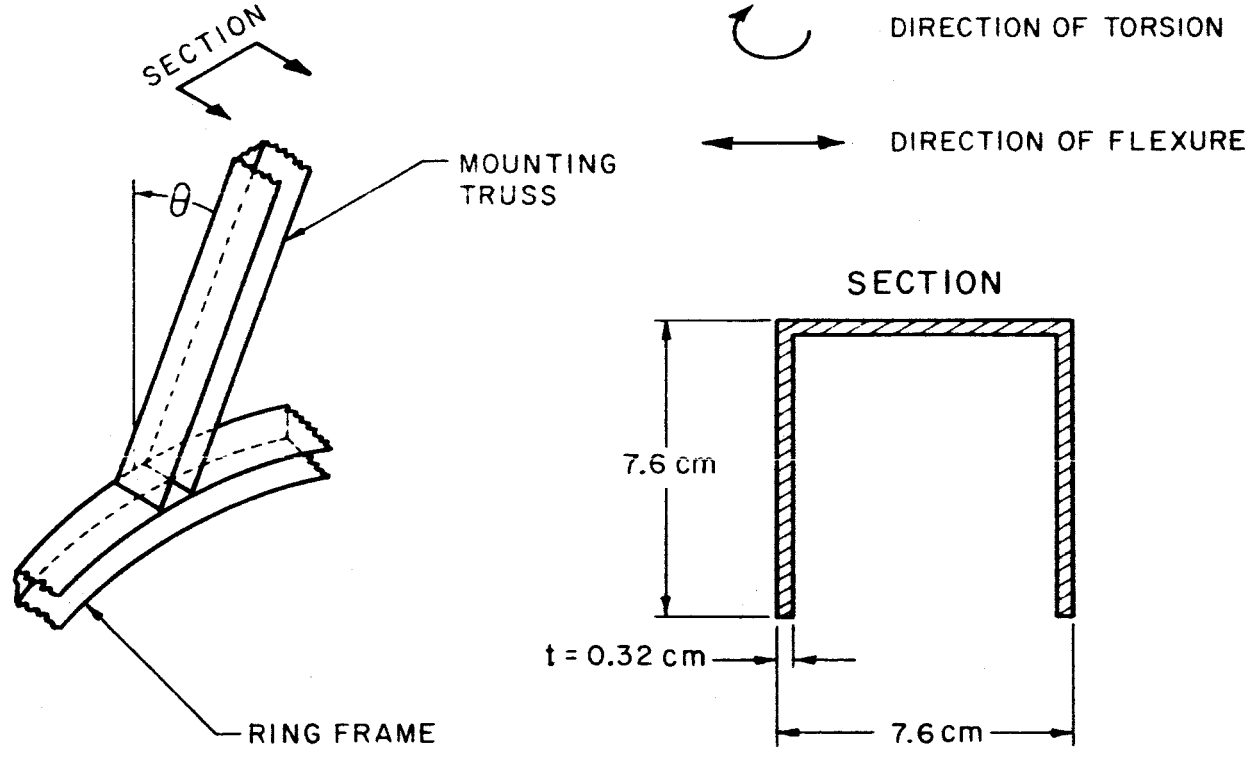

FIG. 5 SINGLE CHANNEL BEAM MODEL OF MOUNTING TRUSS, ITEM (6)

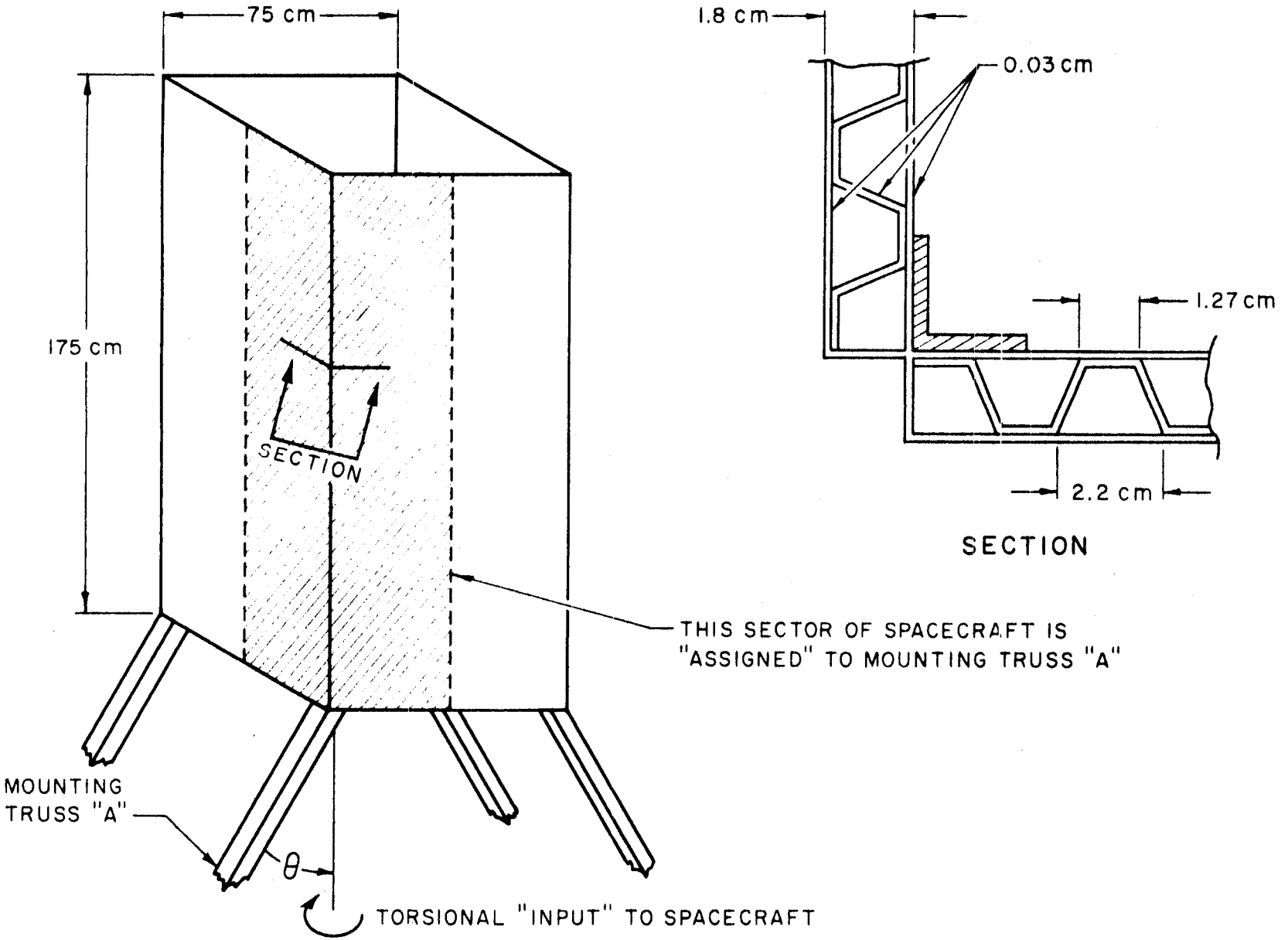

FIG. 6 CONFIGURATION AND CONSTRUCTION OF SPACECRAFT, ITEM (4)

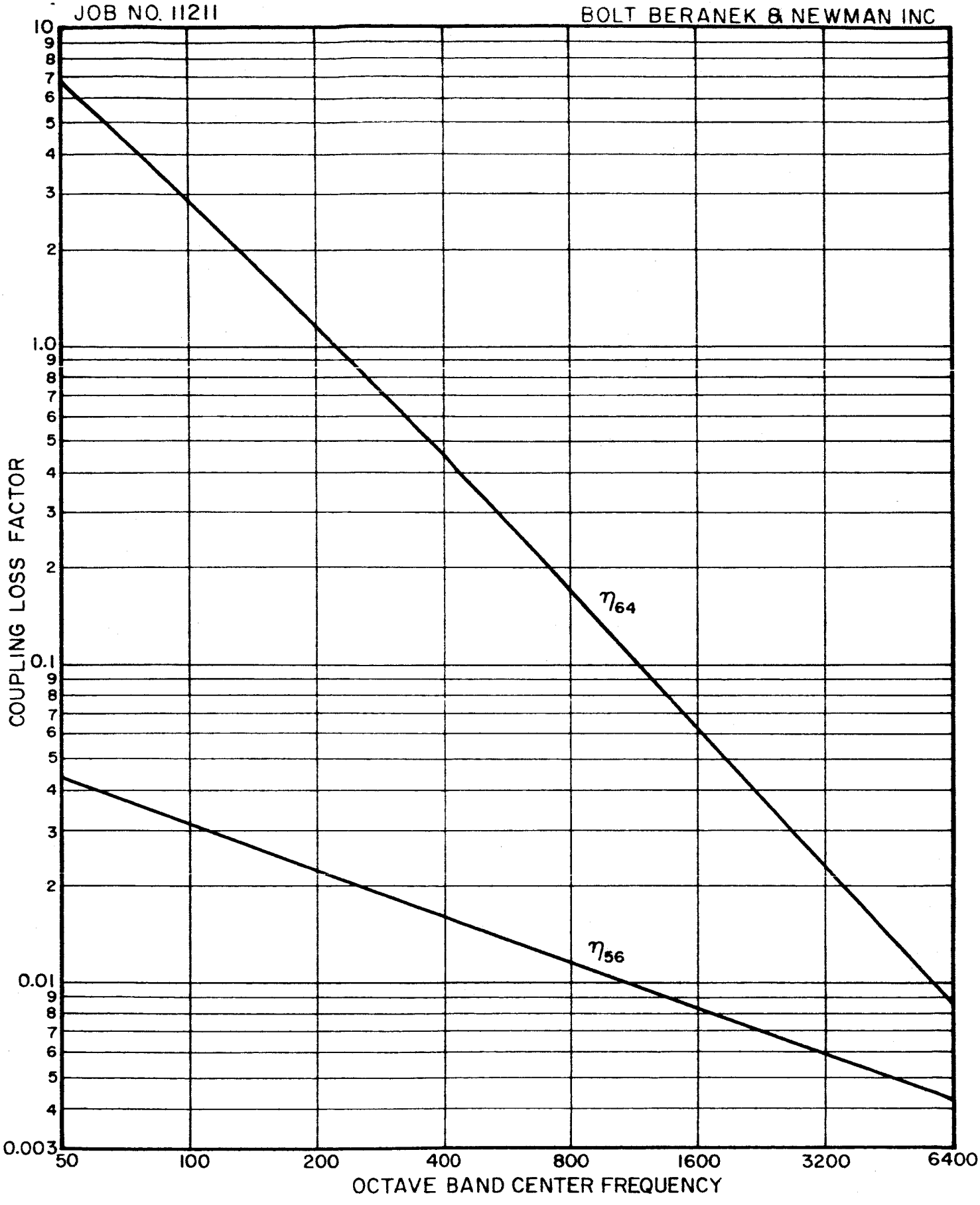

FIG. 7 COUPLING LOSS FACTORS FOR OGO MODEL

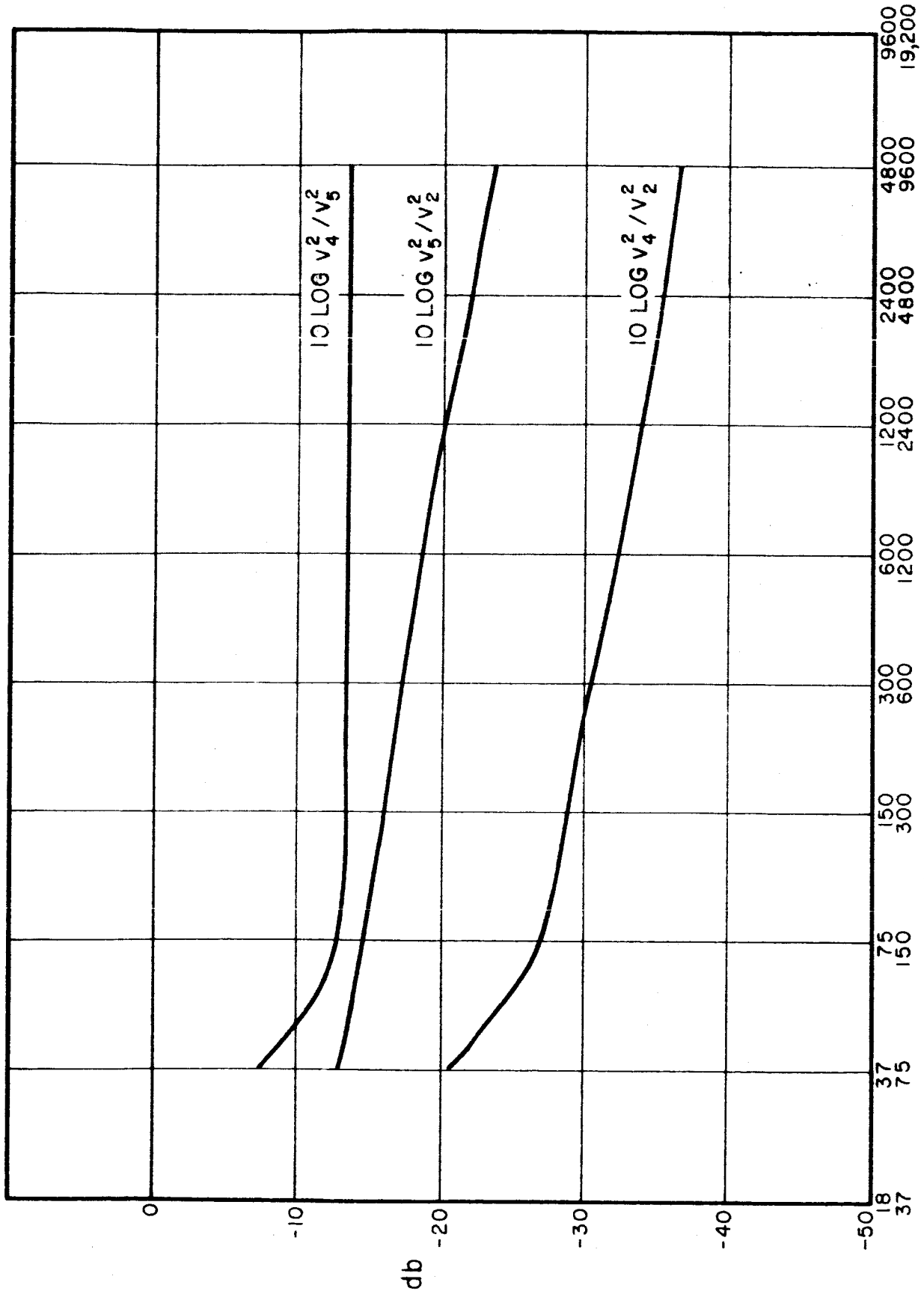

FIG. 8 RESPONSE RATIOS OF OGO ELEMENTS

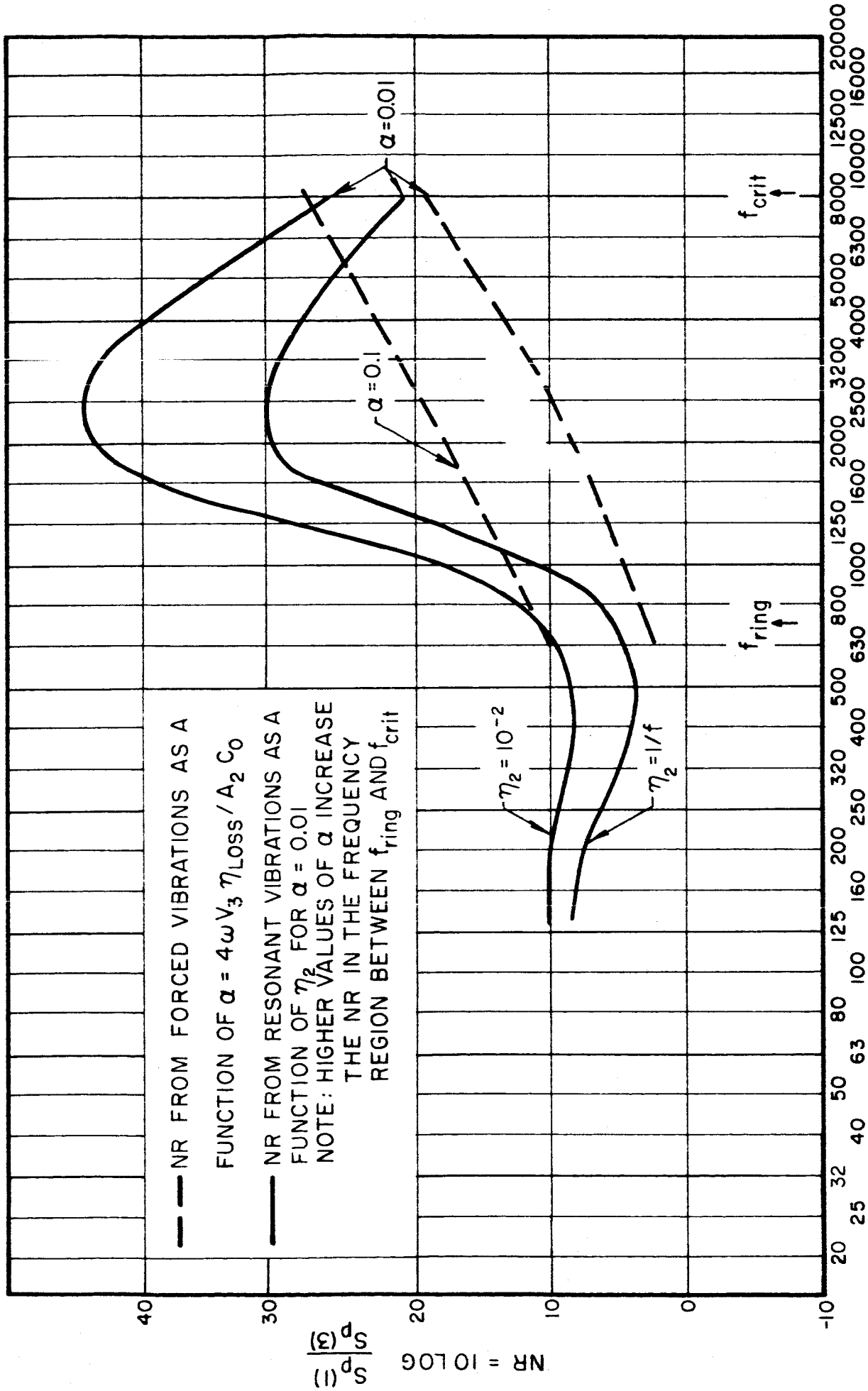

FIG. 9 NOISE REDUCTION OF OGG 0.8 SHROUD